XP-002136343

THE JOURNAL OF BIOLOGICAL CHEMISTRY
© 1997 by The American Society for Biochemistry and Molecular Biology, Inc.
Vol. 272, No. 28, Issue of July 11, pp. 17542–17550, 1997
Printed in U.S.A.

ArgBP2, a Multiple Src Homology 3 Domain-containing, Arg/Abl-interacting Protein, Is Phosphorylated in v-Abl-transformed Cells and Localized in Stress Fibers and Cardiocyte Z-disks*

P.D: 1997
P: 17542 / 17550 (9)

(Received for publication, January 15, 1997, and in revised form, March 24, 1997)

Baolin Wang‡§, Erica A. Golemis¶, and Gary D. Kruh‖**

From the ‡Department of Biology, University of Pennsylvania, Philadelphia, Pennsylvania 19104 and the ¶Basic Science Division and ‖Department of Medical Oncology, Fox Chase Cancer Center, Philadelphia, Pennsylvania 19111

Arg and c-Abl represent the mammalian members of the Abelson family of protein-tyrosine kinases. A novel Arg/Abl-binding protein, ArgBP2, was isolated using a segment of the Arg COOH-terminal domain as bait in the yeast two-hybrid system. ArgBP2 contains three COOH-terminal Src homology 3 domains, a serine/threonine-rich domain, and several potential Abl phosphorylation sites. ArgBP2 associates with and is a substrate of Arg and v-Abl, and is phosphorylated on tyrosine in v-Abl-transformed cells. ArgBP2 is widely expressed in human tissues and extremely abundant in heart. In epithelial cells ArgBP2 is located in stress fibers and the nucleus, similar to the reported localization of c-Abl. In cardiac muscle cells ArgBP2 is located in the Z-disks of sarcomeres. These observations suggest that ArgBP2 functions as an adapter protein to assemble signaling complexes in stress fibers, and that ArgBP2 is a potential link between Abl family kinases and the actin cytoskeleton. In addition, the localization of ArgBP2 to Z-disks suggests that ArgBP2 may influence the contractile or elastic properties of cardiac sarcomeres and that the Z-disk is a target of signal transduction cascades.

Arg and c-Abl are ubiquitously expressed proteins that represent the mammalian members of the Abelson family of non-receptor protein-tyrosine kinases (1, 2). While the central role of the Abl oncoproteins, Gag-Abl and Bcr-Abl, in pre-B lymphomas associated with Abelson murine leukemia virus in mice, and chronic myelogenous leukemia and some forms of acute lymphocytic leukemia in humans (1), respectively, is well established, the normal functions of Arg and c-Abl are less well understood. c-Abl is partially localized in the nucleus (3), and biochemical studies have suggested potential roles for the kinase in cell cycle and transcriptional regulation. c-Abl has been reported to bind to DNA (4), is differentially phosphorylated during the cell cycle (5), associates with the retinoblastoma protein (6), and phosphorylates the COOH-terminal domain of RNA polymerase II (7). In agreement with the biochemical studies that suggest a nuclear function for c-Abl, overexpression of the kinase has been reported to inhibit growth by causing cell cycle arrest (8, 9). In addition, a role for c-Abl in the stress response to DNA damage is indicated by the observations that it is activated by ionizing radiation and alkylating agents, and that c-Abl-deficient cells fail to activate the stress-activated protein kinase pathway in response to these agents (10, 11). Arg, in contrast to c-Abl, is detected exclusively in the cytoplasm when examined by indirect immunofluorescence (12), and does not appear to have a nuclear function.

In addition to nuclear functions, increasing evidence suggests that c-Abl and Abl oncoproteins may influence the actin cytoskeleton. Cytoplasmic c-Abl, and the Bcr-Abl and v-Abl oncoproteins, which are exclusively located in the cytoplasm, have been reported to be localized in actin cytoskeletal structures. c-Abl and Bcr-Abl are localized in stress fibers (3, 13, 14), and Bcr-Abl has been reported to colocalize with focal adhesion proteins in a myeloid cell line (15). v-Abl has also been detected in focal adhesions (16). Sequences that mediate the association of c-Abl and Bcr-Abl with F-actin have been mapped to the distal COOH-terminal domain of c-Abl (13, 14). While Arg is located in the cytoplasm, it is not detected in stress fibers (12). However, the proposed Abl F-actin binding sequences are conserved in the Arg COOH-terminal domain, suggesting the possibility that it may also associate with actin under certain conditions.

In addition to subcellular localization studies, a role for Abl family kinases in actin cytoskeletal events has also been suggested by reports describing potential interactions between Abl and proteins that are associated with cytoskeletal signaling cascades. One potential association is $p130^{cas}$, an SH3-containing protein that was originally isolated as a tyrosine-phosphorylated protein in v-Crk-transformed cells (17, 18). $p130^{cas}$ interacts with FAK[1] (19), is localized in focal adhesions (20) and is phosphorylated in response to integrin engagement (21), suggesting that it is an important component of integrin-mediated cytoskeletal signaling. The observation that $p130^{cas}$ has numerous predicted phosphorylation sites for the Abl kinase (17) and is an *in vitro* substrate of Abl (22), and that the v-Crk adapter protein associates with Arg and c-Abl (23–25), suggest the possibility that Abl family kinases may function as v-Crk effectors that phosphorylate $p130^{cas}$. A more direct link between Abl family kinases and the actin cytoskeleton has been established for Hef1, another SH3-containing protein (26). Hef1 is structurally related to $p130^{cas}$, and its function in cytoskeletal signaling is indicated by its interaction with FAK, the induction of pseudohyphal outgrowth in yeast, and its localization in adhesion plaques. Hef1 associates with v-Abl in cells and is phosphorylated on tyrosine residues in v-Abl-trans-

* This work was supported by Grant CA57273 (to G. D. K.) and Grant CA63366 (to E. A. G.) from the NCI, National Institutes of Health and by an appropriation from the Commonwealth of Pennsylvania to Fox Chase Cancer Center. The costs of publication of this article were defrayed in part by the payment of page charges. This article must therefore be hereby marked "*advertisement*" in accordance with 18 U.S.C. Section 1734 solely to indicate this fact.

§ Current address: Dept. of Molecular Biology and Genetics, Johns Hopkins University School of Medicine, Baltimore, MD 21205.

** To whom correspondence should be addressed: Fox Chase Cancer Center, 7701 Burholme Ave., Philadelphia, PA 19111.

[1] The abbreviations used are: FAK, focal adhesion kinase; SH3, Src homology 3; GST, glutathione *S*-transferase; PCR, polymerase chain reaction; PAGE, polyacrylamide gel electrophoresis; PBS, phosphate-buffered saline; PBST, PBS/Tween 20; kb, kilobase pair(s).

This paper is available on line at http://www.jbc.org

BNSDOCID: <XP___2136343A__I_>

formed fibroblasts. Other potential associations between Abl kinases and components of the actin cytoskeleton include the focal adhesion proteins FAK, paxillin, vinculin, talin, and tensin, which have been reported to be constitutively phosphorylated on tyrosine residues in Bcr-Abl-transformed myeloid cells (15). Finally, 3BP-1, a protein isolated using the Abl SH3 domain as a probe (27), has been shown to have GTPase-activating protein activity for Rac-related small GTP-binding proteins that are involved in regulating the actin cytoskeleton (28). Although these observations support the idea that c-Abl has a role in signaling to the actin cytoskeleton, none of the previously implicated proteins have been demonstrated to be both localized in stress fibers and to directly association with c-Abl. This suggests that Abl family kinases may associate with as yet unidentified cytoskeletal proteins.

In the present study we describe ArgBP2, the second Arg-binding protein that we isolated using a segment of the Arg COOH-terminal domain as bait in the yeast two-hybrid system. ArgBP2 contains three COOH-terminal SH3 domains, several potential phosphorylation sites for c-Abl, and a serine/threonine-rich region. We show that ArgBP2 associates with Arg and v-Abl in living cells and that the endogenous ArgBP2 protein is phosphorylated on tyrosine residues in v-Abl-transformed NIH3T3 cells. ArgBP2 is widely expressed in human tissues and extremely abundant in heart. In epithelial cells ArgBP2 is located in stress fibers and the nucleus, similar to the reported localization of c-Abl. In cardiac muscle cells ArgBP2 is localized in the Z-disks of sarcomeres. Thus, this study suggests that ArgBP2 functions as an adapter protein to assemble signaling complexes in stress fibers, and that ArgBP2 is a potential link between Abl family kinases and the actin cytoskeleton. In addition, ArgBP2 is the first known component of the Z-disk that associates with signaling cascades. The localization of ArgBP2 in Z-disks thus suggests that ArgBP2 may function to influence the contractile or elastic properties of cardiac sarcomeres, and that the Z-disk may be target of signal transduction cascades.

EXPERIMENTAL PROCEDURES

Cells and Antibodies—COS and PtK2 cells (a gift of Joseph W. Sanger, University of Pennsylvania) were maintained in Dulbecco's modified Eagle's medium containing 10% fetal bovine serum. Native and v-Abl-transformed NIH3T3 cells were maintained in Dulbecco's modified Eagle's medium containing 10% calf serum. Sf9 cells (PharMingen) were grown in Grace's medium containing 10% fetal bovine serum, 33 mg/ml yeastolate, and 33 mg/ml lactalbumin hydroxylate (Life Technologies, Inc.) at 27 °C. Cardiomyocytes were obtained from 7-day-old chicken embryos and grown on glass coverslips in serum-free M199 medium for 2 days prior to analysis by indirect immunofluorescence. ArgBP2 polyclonal antibody was generated by immunizing rabbits with the first SH3 domain of the protein expressed in bacteria as a GST fusion protein, and prepared using glutathione-Sepharose beads. The polyclonal Arg antibody 0.7CT has been described previously (29). Anti-phosphotyrosine antibody was purchased from Transduction Laboratories, and anti-Myc antibody was purchased from Santa Cruz Biotechnology.

Plasmid Constructions—The bait plasmid used in the two-hybrid screen, pNLex-ArgSH3BR, has been described previously (30). CB6$^+$-ArgBP2A and CB6$^+$-ArgBP2B were prepared by inserting the respective coding sequences, whose 5′-untranslated sequence had been modified by truncation and altered such that the sequence immediately upstream of the initiation ATG conformed to a Kozak consensus sequence, into the *Eco*RI and *Bam*HI sites of the cytomegalovirus promoter-based expression vector CB6$^+$ (a gift of Frank Rauscher, Wistar Institute). A Myc-tagged ArgBP2 cDNA, pJ3M-Myc-ArgBP2, was constructed by first creating an in-frame *Eco*RI site at the second codon and a *Bgl*II site downstream of the stop codon, and inserting this cDNA into the *Eco*RI and *Bgl*II sites of pJ3M (a gift of Jonathan Chernoff, Fox Chase Cancer Center). DNA fragments encoding each of the ArgBP2 SH3 domains were generated by PCR and inserted into the *Eco*RI and *Bam*HI sites of pGEX-2T (Pharmacia Biotech Inc.). The pGEx plasmids containing the Arg SH3 binding sites, pGExABS-1, pGExABS-2, and pGExABS-3, and the baculovirus expression vector pVL-ArgIB have been described previously (30). pVL-ArgBP2A was constructed by inserting the ArgBP2A sequence of CB6$^+$-ArgBP2A into the *Eco*RI and *Bgl*II sites of pVL1393 (PharMingen). All constructs prepared using PCR products or double-stranded oligonucleotides were confirmed by nucleotide sequence analysis.

Yeast Two-hybrid Screen—A genetic screen using the yeast two-hybrid system was performed as described previously (30, 31). The bait plasmid, pNLex-ArgSH3BR, was described previously (30), and the human brain interaction library was a gift of Roger Brent (Massachusetts General Hospital). The specificity of interaction of candidate plasmids with pNLexArgSH3BR was tested by retransformation of positive clones into yeast harboring either the Arg bait plasmid or several unrelated bait plasmids. Nucleotide sequence analysis of cDNA inserts was performed using an Applied Biosystems automated sequencer.

RNA Blot Analysis and cDNA Library Screening—Filters containing poly(A)$^+$ RNAs prepared from various human tissues (CLONTECH) were hybridized with a radiolabeled ArgBP2A probe as described previously (30). ArgBP2 cDNA clones were isolated by plaque hybridization from a human heart cDNA library (Stratagene) as described previously (30). DNA probes were prepared using [^{32}P]dCTP and a random priming kit (Amersham). Filters were preincubated for at least 1 h at 65 °C in hybridization solution (80 mM Tris-HCl, pH 8.0, 4 mM EDTA, 0.6 M NaCl, 0.1% SDS, 10 × Denhardt's solution, 100 μg/ml denatured salmon sperm DNA). The filters were then incubated overnight at 65 °C with the radiolabeled probe in hybridization solution, washed three times with 0.1 × SSC, 0.1% SDS at 65 °C, and analyzed by autoradiography.

In Vitro Binding Assays—Solution binding assays used to analyze the interaction of GST fusion proteins with proteins expressed in COS or Sf9 cells were performed as described previously (30). GST fusion proteins were expressed in bacteria and purified using glutathione-agarose beads. Proteins were expressed in baculovirus or COS cells as described previously (30). Binding assays were performed by incubating 5 μg of GST fusion proteins (conjugated to glutathione-Sepharose beads) proteins with lysates of Sf9 cells (100 μg) or COS cells (1 mg) in 500 μl of lysis buffer (50 mM HEPES, pH 7.4, 150 mM NaCl, 10% glycerol, 1% Triton X-100, 1 mM EDTA, 10 mM NaF, 1 mM sodium orthovanidate, 1 mM phenylmethylsulfonyl fluoride, 10 μg/ml aprotinin, 10 μg/ml leupeptin). Reactions were allowed to proceed for at least 2 h at 4 °C with constant rotation. Glutathione-agarose beads (15 μl) (Pharmacia) were then added, and the bound proteins were washed four times with 1 ml of incubation buffer (lysis buffer containing 0.1% Triton X-100). Proteins were eluted from the beads with Laemmli sample buffer (32), separated by SDS-PAGE, and detected by immunoblotting with appropriate antibodies.

Transfection of COS and PtK2 Cells and Infection of Sf9 Cells—COS cells were transfected using the DEAE-dextran method as described (33). Cells (1.6 × 10^6) were seeded in 100-mm dishes and transfected the following day with 3 μg of plasmid DNA. After 2.5 h of incubation at 37 °C, growth medium containing 10% Me_2SO was added for 1 min. The dishes were then washed twice with growth medium and incubated in growth medium for 36–60 h. PtK2 cells were transfected using LipofectAMINE (Life Technologies, Inc.) according to the specifications of the manufacturer. Baculoviruses were obtained by cotransfection of Sf9 cells with plasmid constructs and gold-baculovirus (PharMingen). Sf9 cells (2 × 10^6) were infected in 60-mm dishes using 50 μl of baculovirus stocks and then incubated for 36–60 h.

Immunoprecipitation and Immunoblot Analysis—Cells were washed in ice-cold phosphate-buffered saline (PBS) and lysed in 1 ml of lysis buffer. Cell debris was removed by centrifugation at 14,000 rpm for 10 min at 4 °C. Cell lysate (2 mg for COS cells and 300 μg for Sf9 cells) was incubated for 2 h at 4 °C with 1–3 μl of antiserum or monoclonal antibody. For immunoprecipitations using the murine monoclonal antibody, after a 1-h incubation anti-mouse IgG secondary antibody (Boehringer Mannheim) was added. Protein G-bound Sepharose beads (30 μl of a 50% suspension, Pharmacia) were then added, and the suspension was incubated at 4 °C for 30 min with constant rotation. The beads were then washed four times with 1 ml of incubation buffer, and the proteins were eluted with Laemmli sample buffer. Eluted proteins were analyzed by SDS-PAGE and immunoblotting with appropriate antibodies.

For immunoblot analysis, proteins separated by SDS-PAGE were transferred to nitrocellulose filters. Filters were blocked with PBS, 0.1% Tween 20 (PBST) containing 5% nonfat dry milk for 1 h at room temperature. After a brief rinse with PBST, the filters were incubated with appropriate antibodies in PBST, 1% bovine serum albumin for 1 h. The filters were then washed with PBST and incubated with horserad-

BNSDOCID: <XP___2136343A__I_>

ish peroxidase-conjugated anti-mouse or anti-rabbit IgG secondary antibodies (1:5000 in PBST, 1% bovine serum albumin) for 40 min. The filters were washed extensively with PBST followed by PBS and developed with an ECL kit (Amersham).

Immunofluorescence—PtK2 cells were grown on glass coverslips for at least 2 days (collagen-coated coverslips were used in experiments to detect the endogenous protein). For transfection experiments 1 μg of plasmid DNA was used, and the cells were analyzed 2 days later. Cells were fixed using PBS, 4% paraformaldehyde (pH 8.0) for 15 min and permeabilized with PBS, 0.2% Triton X-100 for 5 min. Chicken cardiomyocytes (5×10^4) were grown on glass coverslips in 35-mm dishes for 36 h, and fixed and permeabilized at room temperature for 2 min with acetone:methanol (1:1). PtK2 cells and cardiomyocytes were then washed twice with PBS and incubated for 1 h with 150 μl of PBS, 1% bovine serum albumin, 4% goat serum (PBSBG) containing either preimmune, anti-ArgBP2 polyclonal antibody or anti-Myc monoclonal antibody at a dilutions of 1:1000. After two washes with PBS, the cells were incubated for 1 h with PBSBG containing fluorescein isothiocyanate-conjugated goat anti-rabbit or anti-mouse IgG secondary antibody (Vector) (1:250 dilution) and rhodamine-conjugated phalloidin (Molecular Probes) (1:100 dilution). The cells were then washed three times with PBS, and the coverslips were mounted on glass slides using Vectashield mounting fluid (Vector). Imaging was accomplished using a Bio-Rad confocal microscope with a 60× power lens.

RESULTS

Isolation of ArgBP2 Using the Yeast Two-hybrid System—A segment of the Arg COOH-terminal domain that contains three SH3 binding sites (23) was used as a bait in the yeast two-hybrid system to identify Arg-interacting proteins. A human brain cDNA library was used in the screen, because Arg is well expressed in brain (29) and genetic evidence in *Drosophila* suggests that Abl family kinases may play a role in central nervous system development (34). Four clones that specifically interacted with the bait were identified. Nucleotide sequence analysis revealed that three of the clones contained overlapping sequences of a cDNA denoted ArgBP2 (Arg-binding protein 2). The largest ArgBP2 insert contained a 250-amino acid open reading frame, followed by a stop codon and 250 base pairs of 3′-untranslated sequences. Additional cDNA clones were isolated from a human heart cDNA library by plaque hybridization using an ArgBP2 cDNA insert as the radiolabeled probe. Several cDNA clones were characterized and nucleotide sequence analysis revealed that they represented two distinct classes of ArgBP2 cDNAs (Fig. 1). Analysis of one class of cDNAs (five clones), designated ArgBP2A, indicated that they spanned a total of 5.6 kb. The ArgBP2A sequence encoded a predicted protein of 666 amino acids bordered by in-frame stop codons, indicating that it represented a full-length open reading frame. A second class of cDNAs (two clones), designated ArgBP2B, encoded a partial open reading frame of 618 amino acids followed by a stop codon and 257 base pairs of 3′-untranslated sequence. The partial ArgBP2B predicted protein, which began at the 27th codon of ArgBP2A, was identical to the latter predicted protein over most of its sequences, but differed at its midportion and COOH terminus. To obtain additional 5′ sequences of ArgBP2B, a reverse transcription PCR approach was employed using a primer located 5′ of the upstream in-frame stop codon of ArgBP2A and two nested primers located in the unique ArgBP2B midregion. Nucleotide sequence analysis of the PCR product indicated that the amino-terminal sequence of ArgBP2B was identical to that of ArgBP2A.

ArgBP2 Encodes a Protein with Multiple SH3 Domains—Analysis of the predicted amino acid sequence of ArgBP2A revealed several interesting structural features (Fig. 1, *A* and *B*). The COOH-terminal region of the protein contains three SH3 domains (amino acids 436–484, 511–561, and 614–664), separated by spacers of 26 and 52 amino acids, respectively. Sequences high in proline content are located within the two

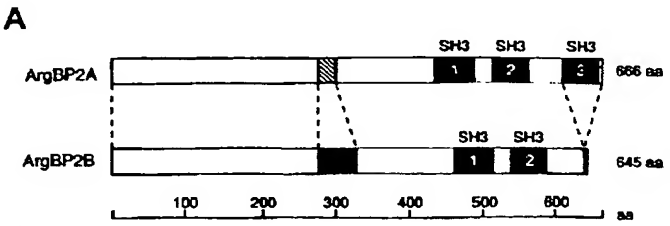

B

```
  1 MRTGRDSQSP DSPKGFRSVR PNLQDKRSPT QSQITVNGNS GGAVSPHSYY
 51 QRPFSPSAYS LPASLNSSIV MQHGTSLDST DTYPQHAQSL DGTTSSSIPL
101 YRSSEEEKRV TVIKAPHYPG IGPVDESGIP TAIRTTVDRP KDWYKTWFKQ
151 IHMVEKPDDD TDKYNTPYIY NAGLYNPFYS AQSHPAAETQ TYRPLSKSHS
201 DNSPEAFKDA SSPVPPPHVP PPVPPLRPRD RSSTEKEDWD PPDRKVDYRK
251 FRSEPRSIFE YEPGKSSILQ HERPTDRINP DDIDLEWEPW YKFFSELEPG
301 RPPPKKPLDY VQDHSSGVFN EASLYQSSID RSLERPNSSA SMASDFRKRR
351 KSEPAVGPPR GLGDQSASRT SPGRVDLPGS STTLTKSFTS SSPSSPSRAK
401 DRESPRSYSS TLTDNGRSAP RERRGTPERE KLPAKAVTDF KAQTSKELSP
451 KKGDTVYILR KIDQNWYEGE HHGRVGIFPI SYVEKLTPPE KAQPARPPPP
501 AQPGEIGZAI AKYNFNADTN VELSLRKGDR VILLKRVDQN WYEGKIPGTN
551 RQGIFPVSYV EVVKKNTKGA EDYPDPPIPH SYSSDRIHSL SSHKPQRPVF
601 THENIQGGGE PFQALYNYTP RNEDELELRE SDVIDVMEKC DDGWFVGTSR
651 RTKFFGTFPG NYVKRL
```

C

```
275 PPLPTTPTPV PREPGRKPLS SSRLGEVTGS PSPPPRSGAP TPSSRAPALSPTR 327
641 GTTLT 645
```

FIG. 1. **Structure and predicted amino acid sequence of ArgBP2.** *A*, schematic representation of ArgBP2. *Black boxes* indicate SH3 domains, and the *stippled* and *shaded boxes* in the midregion of the proteins indicate distinct amino acid sequences. *B*, predicted amino acid sequence of ArgBP2A. The SH3 domains are indicated by *horizontal arrows*, potential Arg/Abl phosphorylation sites are indicated by *asterisks*, and a serine/threonine-rich region is *boxed*. ArgBP2A-specific amino acids are *underlined*. Potential SH3 binding sites (PXXP peptides) are located at amino acids 10–13, 213–228, 304–307, 500–503, 774–777, and 695–698. A potential nuclear localization sequence (RKRRK) is located at amino acids 347–351. *C*, ArgBP2B-specific amino acids. ArgBP2B amino acids 275–327 and 641–645 replace 2A amino acids 275–302 and 616–666, respectively. PXXP motifs are located in the 2B-specific sequence at amino acids 275–283, 285–288, and 305–308.

spacers (PARPPPP and PDPPIP, respectively). These sequences could potentially form turns in the secondary structure of the protein that might function to permit simultaneous binding of distinct proteins to individual SH3 domains. Comparison of the SH3 domains with each other revealed that the first and second domains were highly related, sharing 61% amino acid identity. In contrast, the third SH3 domain shared only 29% and 33% amino acid identity with the first and second SH3 domains, respectively. Comparison of the ArgBP2 SH3 domains with those of other proteins proved quite interesting (Table I). Among the most highly related SH3 domains were those of proteins with functions associated with the cytoskeleton. These proteins included Vav (35, 36), Grb-2 (37), nebulin (38), myosin IC (39), ABP-1 (40), and cortactin (41). The ArgBP2 SH3 domains were also closely related to SH3 domains that we had found previously to bind to the Arg proline-rich sequences, including the SH3 domain of ArgBP1/Abi-2, a protein isolated with the same bait used in the present study (30), and the SH3 domains of the adaptor protein Grb2 (23). These observations suggested that ArgBP2 might have a cytoskeletal function, and that the Arg proline-rich sequences were specific for structurally related SH3 domains.

BNSDOCID: <XP___2136343A__I_>

TABLE I
Similarity of the ArgBP2 SH3 domains to those of other proteins

ArgBP2 SH3 domain	Protein	Identity
		%
SH3–1	Vav (COOH-terminal)	55
	Grb2 (NH_2-terminal SH3)	51
	Myosin IC heavy chain	46
	ArgBP1/Abi-2	44
	Lasp-1	44
	Nebulin	43
	$p40^{phox}$	42
	Grb2 (COOH-terminal SH3)	41
SH3–2	Vav (COOH-terminal)	51
	Vav (NH_2-terminal)	46
	Grb2 (NH_2-terminal SH3)	41
	ArgBP1/Abi-2	39
	Myosin IC heavy chain	37
	$p40^{phox}$	37
	Nebulin	35
	ABP1	34
SH3–3	Vav (COOH-terminal)	51
	ArgBP1/Abi-2	47
	Myosin IC heavy chain	45
	HS1	45
	Abi-1	43
	Lasp-1	41
	ABP1	40
	Cortactin	39

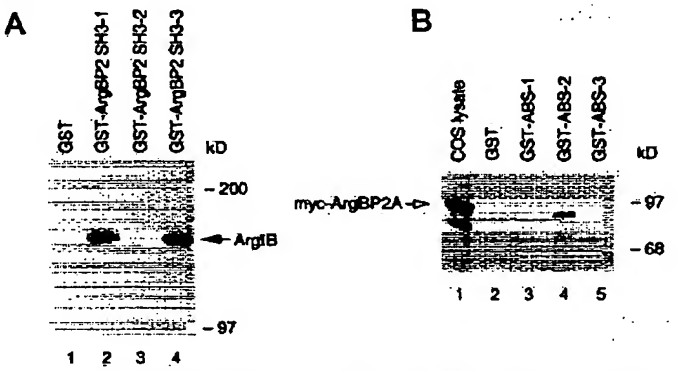

FIG. 2. **Analysis of the mechanism of ArgBP2 binding to Arg.** *A*, analysis of ArgBP2 SH3 domain binding to Arg. Lysates prepared from Sf9 cells infected with an ArgIB baculovirus were incubated with ArgBP2 SH3 domains expressed as GST fusion proteins or control GST protein. Bound proteins were eluted and analyzed by 6% SDS-PAGE and immunoblotting with anti-Arg antibody. The *arrow* indicates the position of ArgIB. *B*, analysis of Arg proline-rich motif binding to ArgBP2A. Lysates prepared from COS cells transfected with pJ3M-Myc-ArgBP2A (*lane 1*) were incubated with GST (*lane 2*) or Arg SH3 binding sites expressed as GST fusion proteins (*lanes 3–5*). Bound proteins were eluted, separated by 8% SDS-PAGE, and immunoblotted with anti-Myc antibody. The *open arrow* indicates the position of Myc-ArgBP2A.

Several other structural features were identified in ArgBP2. Five tyrosine residues are located in sequences that conform to the suggested consensus peptide for the c-Abl tyrosine kinase (YXXP) (42). Four of these tyrosine residues are located in the NH_2-terminal region of the protein, at amino acids 50, 59, 164, and 175. The fifth potential phosphorylation site is located in the spacer region between the second and third SH3 domains, at amino acid 573. The high degree of amino acid identity between the Arg and c-Abl tyrosine kinase domains (94% identity) (2) suggests that these tyrosine residues might also be potential Arg phosphorylation sites. A serine/threonine-rich region in ArgBP2 is located just amino-terminal of the SH3 domains (amino acids 379–413). Serine and threonine residues comprise 56% of this stretch of 34 amino acids. A potential nuclear localization sequence (RKRRK) is located amino-terminal of the serine/threonine-rich region, at amino acids 347–351. Finally, ~10 proline-rich sequences that conform to the PXXP motif found in SH3 binding sites (43) are scattered throughout the protein, including the previously mentioned proline-rich sequences in the SH3 spacer regions. A particularly prominent proline-rich sequence is located between amino acids 213–228, in which 10 of 16 amino acids are proline residues. Data base comparison indicated that a 150-amino acid peptide isolated from gall bladder (44) is 92% identical to ArgBP2 amino acids 136–274.

The ArgBP2B coding sequence differed from that of 2A in two regions. A 28-amino acid stretch of ArgBP2A (amino acids 275–302) is replaced in 2B by a distinct 53-amino acid sequence (2B amino acids 275–327, Fig. 1*C*) that is highly rich in proline residues (28%). Several PXXP motifs are found in this sequence. In addition, the COOH-terminal sequences of ArgBP2A that encode nearly the entire third SH3 domain (amino acids 616–666) is replaced in 2B by 5 distinct amino acids (2B amino acids 641–545). The presence of distinct 2B sequences in the midportion of the protein was confirmed by a reverse transcription PCR approach using a 3′ primer located in the sequence encoding the first SH3 domain and a 5′ primer located just upstream of the unique midportion sequences. Two size classes of PCR fragments were obtained using cDNA prepared from human heart as template. Nucleotide sequence analysis of the two PCR products revealed the expected 2A and 2B sequences, confirming that 2A and 2B represent distinct transcripts.

The ArgBP2 SH3 Domains Have Distinct Specificities for the Arg Proline-rich Motifs—The molecular basis of the ArgBP2 interaction with Arg was examined in detail. We first determined which of the three ArgBP2A SH3 domains bind to Arg. One of the three original activation domain fused ArgBP2A clones contained all three COOH-terminal SH3 domains, whereas two other clones were truncated at their amino termini such that they contained only the third or second and third SH3 domains. Since all three clones interacted with the Arg bait, we concluded that at least the third SH3 domain binds to Arg proline-rich sequences. To confirm that the third SH3 domain mediates binding and to determine if other SH3 domains also bind, each of the three SH3 domains was expressed in bacteria as GST fusion proteins and used in *in vitro* binding experiments. Lysates prepared from Sf9 cells infected with an ArgIB recombinant baculovirus was incubated with each of the three GST-SH3 fusion proteins conjugated to glutathione-Sepharose beads, and bound Arg was detected by immunoblotting with anti-Arg antibody. As shown in Fig. 2*A*, ArgIB binding was readily detected for the first and third ArgBP2 SH3 domains, whereas only very modest binding was detected for the second ArgBP2 SH3 domain.

We next determined which of the three Arg proline-rich regions binds to the ArgBP2 SH3 domains. A Myc epitope tag was fused to the ArgBP2 amino terminus, and Myc-ArgBP2A was expressed in COS cells. Lysates prepared from the transfected COS cells were incubated with each of the three Arg SH3-binding sites expressed in bacteria as GST fusion proteins, and bound Myc-ArgBP2A was detected by immunoblotting with anti-Myc antibody. Myc-ArgBP2A migrated with an apparent molecular mass of 88 kDa, slightly larger than the calculated size of ~75 kDa (Fig. 2*B*, *lane 1*) (a minor degradation product is also seen). As shown in Fig. 2*B*, binding of Myc-ArgBP2A was detected for the second Arg SH3 binding site, but not for the first or third sites. Together these experiments indicate that the second proline-rich motif of Arg binds to the first and third ArgBP2 SH3 domains. A region in the c-Abl COOH-terminal domain, whose location is analogous to

BNSDOCID: <XP___2136343A__I_>

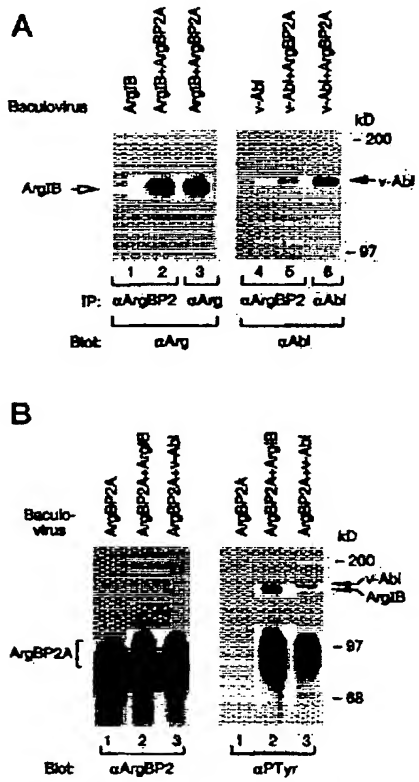

FIG. 3. **Arg and v-Abl associate with and phosphorylate ArgBP2 in living cells.** *A*, association of ArgBP2 with Arg and v-Abl. *Left panel*, immunoprecipitates were prepared from lysates of Sf9 cells infected with ArgIB (*lane 1*) or ArgIB and ArgBP2A baculoviruses (*lanes 2* and *3*) and analyzed by SDS-PAGE and immunoblotting with anti-Arg antibody. *Right panel*, immunoprecipitates were prepared from Sf9 cells infected with v-Abl (*lane 4*) or v-Abl and ArgBP2A baculoviruses (*lanes 5* and *6*) and analyzed by 6% SDS-PAGE and immunoblotting with anti-Abl antibody. The *open* and *closed arrows* indicate the positions of ArgIB and v-Abl, respectively. The positions of prestained molecular size markers are shown to the *right*. *B*, phosphorylation of ArgBP2A by ArgIB and v-Abl. Lysates prepared from Sf9 cells infected with ArgBP2A (*lanes 1*), ArgBP2A and ArgIB (*lanes 2*), or ArgBP2A and v-Abl baculoviruses (*lanes 3*) were analyzed by 8% SDS-PAGE and immunoblotting with either anti-ArgBP2 (*left*) or anti-Tyr(P) antibodies (*right*). The positions of ArgBP2A, ArgIB, and v-Abl are indicated. The positions of prestained molecular size markers are shown to the *right*.

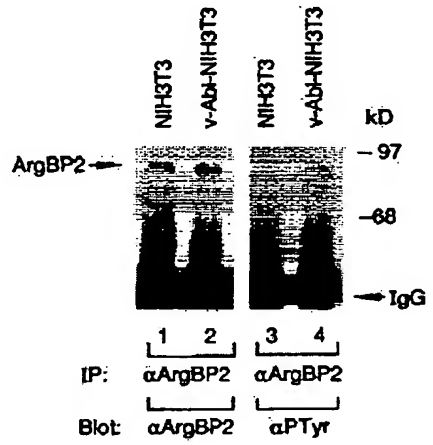

FIG. 4. **ArgBP2 is phosphorylated on tyrosine in v-Abl-transformed NIH3T3 cells.** Lysates (2 mg) prepared from control NIH3T3 cells (*lanes 1* and *3*) or v-Abl-transformed NIH3T3 cells (*lanes 2* and *4*) cells were incubated with 2 μl of anti-ArgBP2 antibody, and immunocomplexes were precipitated with Gamma-bind protein G-agarose beads. The immunoprecipitated proteins were resolved by 8% SDS-PAGE, transferred to nitrocellulose membrane, and immunoblotted with either anti-ArgBP2 (*left*) or anti-Tyr(P) (*right*) antibodies. The positions of ArgBP2 and IgG are indicated by *arrows*. The positions of prestained molecular size markers are shown to the *right*.

that of the Arg SH3 binding region, also harbors three conserved SH3 binding sites that are nearly identical to those of the Arg (25). Similar to Arg, when each of the three c-Abl proline-rich sequences were analyzed for binding to ArgBP2, binding was only detected for the second SH3 binding site (data not shown).

Arg and v-Abl Associate with and Phosphorylate ArgBP2 in Living Cells—The association of ArgBP2A with Arg in living cells was examined in coinfected Sf9 cells. As shown in Fig. 3*A* (*left*), ArgIB was readily detected in anti-ArgBP2 immunoprecipitates prepared from cells coinfected with ArgBP2A and ArgIB baculoviruses, but not in cells infected with ArgIB baculovirus alone. Similarly, the v-Abl oncoprotein was detected in anti-ArgBP2 immunoprecipitates prepared from Sf9 cells coinfected with ArgBP2A and v-Abl baculoviruses, but not in cells infected with a v-Abl baculovirus alone (Fig. 3*A*, *right*). These experiments indicated that the full-length ArgBP2A protein interacts with Arg and v-Abl in living cells. Although this interaction was readily detectable in cells that overexpress Abl family kinases and ArgBP2, we were unable to detect the association in native mammalian cells, possibly owing to the very low levels of Arg and c-Abl proteins in the cell and limitations in our immunological reagents.

In view of the presence in ArgBP2 of potential Arg/Abl phosphorylation sites, the possibility that ArgBP2 is a substrate of Abl family kinases was also examined. Lysates prepared from Sf9 cells infected with an ArgBP2A baculovirus alone, or coinfected with ArgBP2A and Arg or v-Abl baculoviruses, were analyzed by immunoblotting with either anti-ArgBP2 or anti-Tyr(P) antibodies. As shown in Fig. 3*B* (*left*), ArgBP2A expressed in Sf9 cells migrated with an apparent molecular mass of ~88 kDa, similar to the size observed in transfected COS cells (the lower molecular mass bands are degradation products). Phosphorylation of ArgBP2 on tyrosine residues in cells coinfected with Arg or v-Abl baculoviruses, but not in cells infected with the ArgBP2 baculovirus alone, was readily detected in the anti-phosphotyrosine immunoblot (Fig. 3*B*, *right*). As expected for this covalent modification, a slight reduction in the SDS-PAGE mobility of phosphorylated ArgBP2A was detected in both anti-ArgBP2 and anti-Tyr(P) immunoblots. ArgIB and v-Abl are detected in the anti-Tyr(P) immunoblot owing to their *in vivo* phosphotyrosine content (Arg, like c-Abl, is phosphorylated on tyrosine residues when expressed at high levels in Sf9 cells).

Endogenous ArgBP2 Is Phosphorylated on Tyrosine Residues in v-Abl-transformed Cells—Based upon the observation that v-Abl associates with and phosphorylates ArgBP2 in infected Sf9 cells, we reasoned that if ArgBP2 is a physiological substrate of c-Abl the endogenous protein should be phosphorylated on tyrosine residues in cells harboring an activated Abl oncoprotein. This possibility was examined by analyzing the phosphotyrosine content of endogenous ArgBP2 in NIH3T3 cells transformed by the v-Abl oncoprotein. ArgBP2 in native and v-Abl-transformed NIH3T3 cells was immunoprecipitated with anti-ArgBP2 antiserum and immunoblotted with either anti-ArgBP2 or anti-Tyr(P) antibodies. As shown in Fig. 4 (*left*), ArgBP2 was readily detected in the anti-ArgBP2 immunoblot, and migrated with an apparent molecular weight similar to that of the transfected human protein. When immunoblotted with anti-Tyr(P) antibody, ArgBP2 was consistently detected in the v-Abl-transformed cells, but not the control untransfected

BNSDOCID: <XP___2136343A__I_>

NIH3T3 cells (Fig. 4, *right*), indicating that it is phosphorylated on tyrosine residues in v-Abl-transformed cells. Tyrosine phosphorylation of ArgBP2 was not detected when nonimmunoprecipitated lysates were analyzed with anti-Tyr(P) antibody (data not shown), suggesting either that ArgBP2 is not abundant in NIH3T3 cells or that it is not highly tyrosine-phosphorylated. Consistent with the former possibility, when nonimmunoprecipitated lysates were immunoblotted with anti-ArgBP2 antibody, the ~88-kDa ArgBP2 band was not intense (data not shown). In addition to the expected 88-kDa protein product, a second band of ~40 kDa was also detected in immuoblots of NIH3T3 cells. In view of the numerous ArgBP2 transcript species identified in the RNA blot (see below), it is possible that this band represents an ArgBP2 isoform. However, because the antibody used in these experiments was raised against an SH3 domain, we cannot exclude the possibility that the 40-kDa band represents a cross-reacting protein).

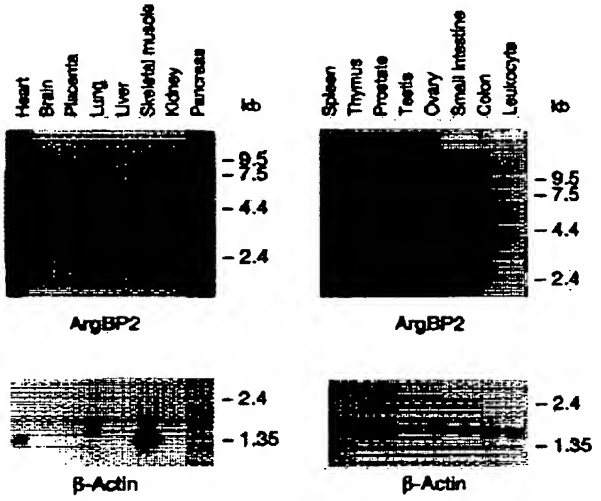

FIG. 5. **Tissue distribution of ArgBP2.** Filters containing poly(A)$^+$ RNA prepared from various human tissues were hybridized with a radiolabeled ArgBP2 (*top*) or β-actin probe (*bottom*). The positions of size markers are shown to the *right*. A segment of the ArgBP2A cDNA (nucleotides 2016–3045) was used as the probe.

ArgBP2 Is Widely Expressed in Human Tissues and Extremely Abundant in Heart—To gain insight into the biological functions of ArgBP2, its expression pattern in human tissues was examined by Northern blot analysis. As shown in Fig. 5, ArgBP2 transcripts were detected in each of 16 poly(A)$^+$ RNA samples prepared from human tissues, with the exception of peripheral leukocytes. ArgBP2 transcript was extremely abundant in heart, in which it was expressed at levels ~50–200-fold higher than other tissues. Several size classes of transcripts were observed, consistent with the isolation of more than one class of ArgBP2 cDNAs. A 4.4-kb transcript was detected in most tissues, with the exception of heart, brain, kidney, and spleen. In addition, transcripts of 5 kb (small intestine, heart, pancreas, and thymus) and 5.8 kb (colon, heart, spleen, prostate, testis, and ovary) were observed. A distinct transcript of 6.6 kb was detected in brain. (The sizes of the heart ArgBP2 transcripts were determined using reduced exposure times).

ArgBP2 Is Localized in the Z-disks of Cardiac Myocytes—The subcellular localization of ArgBP2 was examined to gain insight into its possible physiological functions. Since the RNA blot analysis indicated that ArgBP2 transcript is extremely abundant in heart, we first analyzed subcellular localization in cardiac muscle cells. Primary cardiac myocytes obtained from 7-day-old chicken embryos were grown on coverslips, and the subcellular localization of endogenous ArgBP2 was analyzed by indirect immunofluorescence using anti-ArgBP2 polyclonal antibody. As shown in Fig. 6 (*right panel*), ArgBP2 was readily detected in cardiocytes. The periodic staining pattern is characteristic of localization to the Z-disks of cardiac myofibrils. In contrast, when preimmune serum was used, almost no staining was detected (*left panel*). This staining pattern indicates that ArgBP2 has a specialized function associated with the contractile apparatus of cardiac muscle cells.

ArgBP2 Is Localized in Stress Fibers and the Nucleus in PtK2 Cells—While most abundant in heart, ArgBP2 transcript was also detected in a wide range of other human tissues. Based upon the localization of ArgBP2 in cardiocyte Z-disks, and the similarity of its SH3 domains to those found in proteins associated with the cytoskeleton, we reasoned that its nonmuscle function might be related to actin cytoskeletal structures, such as stress fibers. To examine ArgBP2 subcellular localization in nonmuscle cells, immunostaining experiments were therefore

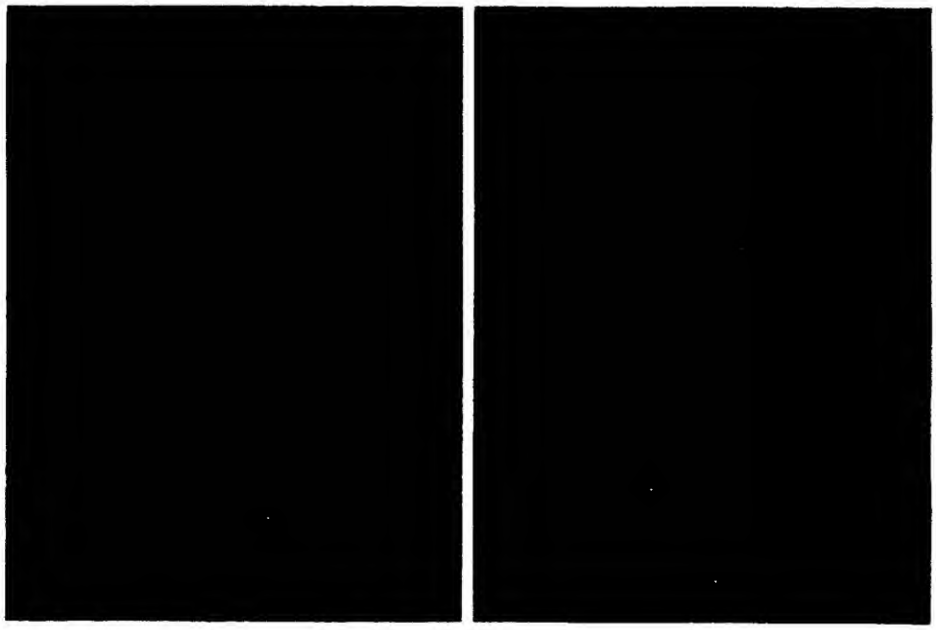

FIG. 6. **Subcellular localization of ArgBP2 in primary chicken cardiomyocytes.** Cardiomyocytes from 7-day-old chicken embryos were grown on glass coverslips and analyzed by indirect immunofluorescence using anti-ArgBP2 (*right*) or preimmune (*left*) sera.

BNSDOCID: <XP__2136343A__I_>

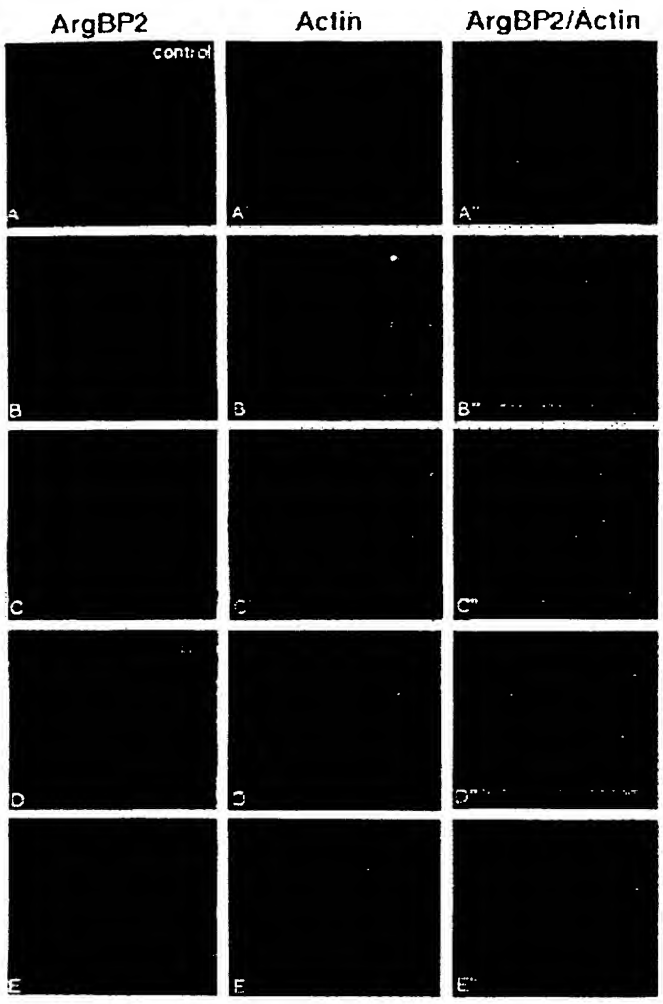

FIG. 7. **Subcellular localization of ArgBP2 in PtK2 kidney epithelial cells.** *Left column*, indirect immunofluorescence using preimmune serum (*A*), anti-ArgBP2 serum (*B–D*), or anti-Myc antibody (*E*); *middle column*, actin stained by rhodamine-conjugated phalloidin; *right column*, superimposed images of anti-ArgBP2 and actin staining. *A* and *B*, untransfected PtK2 cells; *C*, PtK2 cells transfected with CB6$^+$-ArgBP2A; *D*, PtK2 cells transfected with CB6$^+$-ArgBP2B; *E*, PTK2 cells transfected with pJ3M-Myc-ArgBP2A. Cells were imaged by confocal microscopy.

performed using PtK2, a marsupial kidney epithelial cell line that is widely used for analysis of the actin cytoskeleton because it has prominent stress fibers. We first examined the localization of the endogenous protein. Fig. 7 shows PtK2 cells stained with either preimmune serum or anti-ArgBP2 serum (*panels A* and *B*, respectively). A filamentous staining pattern characteristic of stress fibers was observed using anti-ArgBP2 antibody. In contrast, only modest nonspecific staining was observed when preimmune serum was used. To further investigate whether ArgBP2 is localized in stress fibers, these structures were revealed in the same cells by staining actin with rhodamine-conjugated phalloidin. Comparison of *panels B* and *B'* shows that anti-ArgBP2 antibody staining colocalized with phalloidin staining (*B"* shows the superimposed anti-ArgBP2 and actin images).

To confirm the localization of ArgBP2 in stress fibers, immunostaining experiments were performed using transfected PtK2 cells and anti-ArgBP2 antibody. *Panel C* shows the staining pattern observed in cells transfected with the ArgBP2A expression vector, CB6$^+$-ArgBP2A. As expected, the staining pattern was similar to that observed for the endogenous protein, except that enhanced staining of stress fibers was observed in association with the higher protein expression levels achieved in transfected cells. The enhanced level of detection revealed a bead-like pattern of ArgBP2A staining in stress fibers. The periodic beaded structures, termed dense bodies, are the structures at which actin filaments are anchored and are thought to be the equivalents of the Z-disks of sarcomeres in striated muscle (45). The specificity of the staining pattern observed with anti-ArgBP2 antibody was confirmed by analyzing PtK2 cells transfected with pJ3M-Myc-ArgBP2A, a Myc epitope-tagged ArgBP2A expression vector. *Panel E* shows that the immunostaining pattern observed with anti-Myc monoclonal antibody was similar to the pattern observed in transfected and untransfected PtK2 cells using anti-ArgBP2 antibody.

To determine whether the differences in the ArgBP2B coding sequence compared with ArgBP2A influenced its subcellular localization, we analyzed PtK2 cells transfected with the ArgBP2B expression vector, CB6$^+$-ArgBP2B. As shown in *panel D*, ArgBP2B was detected in stress fibers at levels that were similar to those of the transfected ArgBP2A protein. However, in contrast to ArgBP2A, the ArgBP2B isoform was also localized in the nucleus. Thus, in nonmuscle cells, the localization of ArgBP2 in stress fibers and the nucleus is similar to the intracellular distribution reported for c-Abl (3, 14).

DISCUSSION

To identify components of the signal transduction pathways in which Abl family kinases function, we used the yeast two-hybrid screen with a bait consisting of a segment of the Arg COOH-terminal domain that harbors three SH3 binding sites. Using this approach we isolated ArgBP2, an SH3-containing protein that associates with Abl family kinases. ArgBP2 has several recognizable structural motifs, including three SH3 domains, a serine/threonine-rich region, five peptide sequences that conform to the proposed target for the Abl kinase domain, and several proline-rich sequences. ArgBP2 is widely distributed in tissues, and extremely abundant in heart. We demonstrate that in nonmuscle cells the protein is localized in stress fibers, whereas in cardiac cells ArgBP2 is localized exclusively in the Z-disks of sarcomeres. In addition, in nonmuscle cells an ArgBP2 isoform is localized in the nucleus, as well as in stress fibers. The structure and intracellular distribution of ArgBP2, and its association with Abl family kinases, have important implications for its function in signaling cascades that influence the cytoskeleton, as well as for the function of Z-disks in cardiac sarcomeres.

ArgBP2 and Abl Family Kinases—The localization of c-Abl and Abl oncoproteins to stress fibers and the presence in the Abl COOH-terminal domain of an F-actin binding site indicate that the kinase plays a role in signaling to the actin cytoskeleton. However, understanding the function of c-Abl in stress fibers has been limited by the absence of known Abl-interacting proteins located in this intracellular location. The present study suggests that ArgBP2 represents a potential direct link between Abl family kinases and stress fibers. This conclusion is supported by several observations. 1) ArgBP2, like cytoplasmic c-Abl, is localized in stress fibers; 2) ArgBP2 directly associates with Arg and v-Abl in living cells; 3) ArgBP2 is a substrate for Abl family kinases, consistent with the observation that it has several sequences that conform to the suggested peptide target for the Abl kinase; 4) endogenous ArgBP2 is phosphorylated on tyrosine residues in NIH3T3 cells transformed by v-Abl, a dysregulated Abl oncoprotein; and 5) the mechanism of ArgBP2 binding with Abl family kinases is specific (the first and third

BNSDOCID: <XP___2136343A__I_>

ArgBP2 SH3 domains interact with the second of three proline-rich motifs located in the Arg and c-Abl COOH-terminal domains). Together these findings suggest that ArgBP2 is a potential physiological cytoskeletal target for Abl family kinases.

While several reports have suggested potential links between c-Abl and Abl oncoproteins with proteins associated with cytoskeleton signaling cascades, such as the SH3-containing proteins $p130^{cas}$ (17) and Hef1 (26), none of the reported proteins appear to be good candidates for mediating the action of c-Abl in stress fibers. For example, while $p130^{cas}$ contains 12 predicted phosphorylation sites for the c-Abl kinase (42), is an *in vitro* substrate of Abl, and is phosphorylated on tyrosine in cells transformed by v-Crk, an adapter protein that associates with c-Abl and Arg (23–25), a direct association between $p130^{cas}$ and Abl family kinases has not been demonstrated. In addition, $p130^{cas}$ has not been reported to be phosphorylated in Abl oncoprotein-transformed cells and tyrosine phosphorylation of $p130^{cas}$ is not reduced in c-Abl-deficient cells (46). In the case of the $p130^{cas}$-related protein, Hef1, a direct association has been established (26). However, Hef1 is located in adhesion plaques, but not in stress fibers. Other cytoskeletal proteins that have been reported to be phosphorylated in Abl oncoprotein-transformed cells, such as FAK, paxillin, vinculin, tensin, and talin, are components of focal adhesions.

ArgBP2 and the Actin Cytoskeleton—The broad tissue distribution of ArgBP2, and its localization in nonmuscle cells in stress fibers, suggests that it may play a role in signals that regulate the actin cytoskeleton in many cell types. Accumulating evidence indicates that small GTP-binding proteins of the Rho family and the GTPase-activating proteins and nucleotide exchange factors that influence their activities are important regulators of the actin cytoskeleton (47). In addition to small GTP-binding proteins, protein kinases such as FAK and Pak, and lipid kinases such as phosphoinositol 3-kinase, also play important roles in cytoskeletal modeling (48). While progress has been made in understanding the upstream components of signaling cascades that influence the actin cytoskeleton in mammalian cells, little is known about the distal cytoskeletal associations of these cascades outside of the components of focal adhesions. ArgBP2 is a good candidate for such a target. The absence in ArgBP2 of kinase, Dbl homology, or GTPase-activating protein homology domains that are found in the latter signaling proteins, indicates that it is not an upstream component of signaling cascades. Instead, the presence in ArgBP2 of at least three protein interaction motifs suggests that it has complex protein interactions, and supports the idea that it is likely to link upstream signaling components to the actin cytoskeleton. This idea is also supported by the association of ArgBP2 with Arg and v-Abl. In addition, the presence in ArgBP2 of a prominent serine/threonine-rich region raises the possibility that it may also be a target of serine/threonine kinases. Consistent with this possibility, we have found the protein is heavily phosphorylated on serine residues *in vivo*.[2] Together these observations suggest that ArgBP2 may function as an adapter protein to assemble signaling complexes in stress fibers, and that it is likely to associate with signaling proteins in addition to Abl family kinases. Additional studies are in progress to define the proteins that interact with ArgBP2.

ArgBP2 and the Z-disks of Cardiac Muscle Cells—The striking abundance of ArgBP2 transcript in heart, but not skeletal muscle, indicates that it has a specialized function in cardiac muscle. The localization of ArgBP2 to the Z-disks of cardiac sarcomeres further indicates that this specialized function involves this structure. The Z-disk, which is a feature of striated muscle, is a filamentous lattice that defines the ends of the muscle sarcomere, and is important in the transmission of forces between sarcomeres. Z-filaments, the extensions of actin filaments, are anchored at the Z-disk, where they are held in an ordered lattice arrangement by other proteins. The actin-cross-linking protein α-actinin is a principal structural component of the Z-disk that is thought to play an important role in anchoring Z-filaments (49, 50). Other components of the Z-disk of striated muscle include the giant muscle proteins nebulin and titan, whose ends are anchored in the Z-disk (51), the actin-capping protein Cap-Z (52), and the actin-cross-linking protein filamin (53, 54).

ArgBP2 thus joins a small group of proteins that are known to be located at Z-disks. However, with the exception of a nebulin isoform that is restricted in expression to cardiac Z-disks (55), ArgBP2 is the only known Z-disk-associated protein whose expression pattern indicates a special role in cardiac muscle, as opposed to both types of mammalian striated muscle. In addition, ArgBP2 is the first known component of Z-disks that associates with signal transduction cascades. Nebulin and titan are fibrous proteins that have important roles in maintaining the overall architecture of the sarcomere (51), and α-actinin, Cap-Z, and filamin are actin-binding proteins that have structural functions associated with this filament. In contrast, ArgBP2 has neither a conserved actin binding domain, nor highly repetitive motifs, and is therefore unlikely to have either a structural or architectural role. Instead, its multiple SH3 domains and association with Abl family kinases support the idea that the primary role of ArgBP2 involves signaling cascades. The localization of ArgBP2 to Z-disks thus has intriguing implications. It suggests that the Z-disk is a site of biochemical signaling to the sarcomere and that ArgBP2 might function to mediate biochemical signals that could influence the contractile and/or elastic forces in cardiac muscle. In view of these considerations, it is worth noting that in cardiac muscle the tubular invaginations of the sarcolemma that comprise the T system are located at the level of the Z-disk (as opposed to the A-I junction as in mammalian skeletal muscle). Since these tubules are inward extensions of the extracellular space at which excitation is coupled to contraction, it suggests the possibility that ArgBP2 might have a role in signals that arise from the extracellular space.

Nuclear ArgBP2—The localization of an ArgBP2 isoform in the nucleus indicates that the function of ArgBP2 is complex and extends beyond linking upstream cytoplasmic signaling proteins to the actin cytoskeleton. One possibility is that nuclear ArgBP2B might function in a reverse fashion compared with ArgBP2A, by linking signals that arise in the actin cytoskeleton to nuclear events, such as alterations in gene transcription and cell proliferation. Alternatively, nuclear ArgBP2 might participate in F-actin associated mitotic events, such as the formation of cleavage furrows. In view of the nuclear localization of ArgBP2B, it is interesting to note c-Abl is also partially localized in the nucleus (3). Thus the intracellular distribution of ArgBP2 parallels that of c-Abl. Since the first of the two remaining SH3 domains in ArgBP2B can bind to c-Abl, it is possible that nuclear ArgBP2 is a substrate of nuclear c-Abl.

The structure of ArgBP2B differs from that of ArgBP2A in that a 28-amino acid segment located in the midportion of the latter protein is replaced by a 53-amino acid 2B-specific sequence, and that the third SH3 domain of the 2A isoform is absent in ArgBP2B. How these structural differences influence the nuclear distribution of the protein is not clear. While a potential nuclear localization sequence (RKRRK) is present in ArgBP2, it is located in a region that is common to both isoforms, suggesting that either another nuclear localization se-

[2] B. Wang and G. D. Kruh, unpublished observations.

BNSDOCID: <XP___2136343A__I_>

quence is present in the ArgBP2B-specific amino acids, or possibly that the distinct 2A or 2B sequences somehow modify the function of the common nuclear localization sequence. In addition to extending the intracellular distribution of the protein to the nucleus, these differences may influence the spectrum of proteins with which both the nuclear and cytoplasmic isoforms associate. Protein interactions mediated exclusively by the third SH3 domain of ArgBP2A would be lost, and the 2B-specific sequences might mediate distinct associations. The latter possibility is suggested by the presence in the 2B-specific sequence of proline-rich peptides that could function as SH3 binding sites.

Acknowledgments—We thank Dr. Joseph W. Sanger for helpful discussions, for insightful comments regarding the localization and possible functions of ArgBP2, and for critically reviewing the manuscript. We also thank Lena Kotova for technical assistance, Drs. John Burch and Chao-Zhen He for help with culturing chicken cardiocytes, Joanne Estojak for help with the two-hybrid screen, Jonathan Boyd and Marija Helt for assistance with the confocal microscope, and Drs. Jonathan Chernoff and Charles Reichman for critically reviewing the manuscript.

Note Added in Proof—We have become aware of a protein that shares the structural architecture of ArgBP2. SH3P12, a murine protein isolated in a functional screen using SH3 ligands (Sparks, A. B., Hoffman, N. G., McConnell, S. J., Fowlker, D. M. and Kay, B. K. (1996) *Nature Biotech.* **14**, 741–744), is 45% identical to ArgBP2 overall. The SH3 domains of ArgBP2 are 76%, 69%, and 80% identical to those of SH3P12. Sh3P12 may therefore represent either the murine homologue of ArgBP2 or a related protein.

REFERENCES

1. Wang, J. Y. (1993) *Curr. Opin. Genet. Dev.* **3**, 35–43
2. Kruh, G. D., Perego, R., Miki, T., and Aaronson, S. A. (1990) *Proc. Natl. Acad. Sci. U. S. A.* **87**, 5802–5806
3. Van Etten, R. A., Jackson, P., and Baltimore, D. (1989) *Cell* **58**, 669–678
4. Kipreos, E. T., and Wang, J. Y. (1992) *Science* **256**, 382–385
5. Kipreos, E. T., and Wang, J. Y. (1990) *Science* **248**, 217–220
6. Welch, P. J., and Wang, J. Y. (1993) *Cell* **75**, 779–790
7. Baskaran, R., Dahmus, M. E., and Wang, J. Y. (1993) *Proc. Natl. Acad. Sci. U. S. A.* **90**, 11167–11171
8. Mattioni, T., Jackson, P. K., Bchini-Hooft van Huijsduijnen, O., and Picard, D. (1995) *Oncogene* **10**, 1325–1333
9. Sawyers, C. L., McLaughlin, J., Goga, A., Havlik, M., and Witte, O. (1994) *Cell* **77**, 121–131
10. Kharbanda, S., Ren, R., Pandey, P., Shafman, T. D., Feller, S. M., Weichselbaum, R. R., and Kufe, D. W. (1995) *Nature* **376**, 785–788
11. Kharbanda, S., Pandey, P., Ren, R., Mayer, B., Zon, L., and Kufe, D. (1995) *J. Biol. Chem.* **270**, 30278–30281
12. Wang, B., and Kruh, G. D. (1996) *Oncogene* **13**, 193–197
13. McWhirter, J. R., and Wang, J. Y. (1991) *Mol. Cell. Biol.* **11**, 1553–1565
14. Van Etten, R. A., Jackson, P. K., Baltimore, D., Sanders, M. C., Matsudaira, P. T., and Janmey, P. A. (1994) *J. Cell Biol.* **124**, 325–340
15. Salgia, R., Brunkhorst, B., Pisick, E., Li, J. L., Lo, S. H., Chen, L. B., and Griffin, J. D. (1995) *Oncogene* **11**, 1149–1155
16. Rohrschneider, L. R., and Najita, L. M. (1984) *J. Virol.* **51**, 547–552
17. Sakai, R., Iwamatsu, A., Hirano, N., Ogawa, S., Tanaka, T., Mano, H., Yazaki, Y., and Hirai, H. (1994) *EMBO J.* **13**, 3748–3756
18. Sakai, R., Iwamatsu, A., Hirano, N., Ogawa, S., Tanaka, T., Nishida, J., Yazaki, Y., and Hirai, H. (1994) *J. Biol. Chem.* **269**, 32740–32746
19. Polte, T. R., and Hanks, S. K. (1995) *Proc. Natl. Acad. Sci. U. S. A.* **92**, 10678–10682
20. Petch, L. A., Bockholt, S. M., Bouton, A., Parsons, J. T., and Burridge, K. (1995) *J. Cell Sci.* **108**, 1371–1379
21. Nojima, Y., Morino, N., Mimura, T., Hamasaki, K., Furuya, H., Sakai, R., Sato, T., Tachibana, K., Morimoto, C., Yazaki, Y., and Hirai, H. (1995) *J Biol Chem* **270**, 15398–15402
22. Mayer, B. J., Hirai, H., and Sakai, R. (1995) *Curr. Biol.* **5**, 296–305
23. Wang, B., Mysliwiec, T., Feller, S. M., Knudsen, B., Hanafusa, J., and Kruh, G. D. (1996) *Oncogene* **13**, 1379–1385
24. Feller, S. M., Knudsen, B., and Hanafusa, H. (1994) *EMBO J.* **13**, 2341–2351
25. Ren, R., Ye, Z. S., and Baltimore, D. (1994) *Genes Dev.* **8**, 783–795
26. Law, S. F., Estojak, J., Wang, B., Mysliwiec, T., Kruh, G., and Golemis, E. A. (1996) *Mol. Cell. Biol.* **16**, 3327–3337
27. Cicchetti, P., Mayer, B. J., Thiel, G., and Baltimore, D. (1992) *Science* **257**, 803–806
28. Cicchetti, P., Ridley, A. J., Zheng, Y., Cerione, R. A., and Baltimore, D. (1995) *EMBO J.* **14**, 3127–3135
29. Perego, R., Ron, D., and Kruh, G. D. (1991) *Oncogene* **6**, 1899–1902
30. Wang, B., Mysliwiec, T., Krainc, D., Jensen, R. A., Sonoda, G., Testa, J. R., Golemis, E. A., and Krub, G. D. (1996) *Oncogene* **12**, 1921–1929
31. Gyuris, J., Golemis, E., Chertkov, H., and Brent, R. (1993) *Cell* **75**, 791–803
32. Laemmli, U. K., and Eiserling, F. A. (1968) *Mol. Gen. Genet.* **101**, 333–345
33. Morris, J. F., Madden, S. L., Tournay, O. E., Cook, D. M., Sukhatme, V. P., and Rauscher, F. J., 3rd (1991) *Oncogene* **6**, 2339–2348
34. Gertler, F. B., Bennett, R. L., Clark, M. J., and Hoffmann, F. M. (1989) *Cell* **58**, 103–113
35. Hobert, O., Schilling, J. W., Beckerle, M. C., Ullrich, A., and Jallal, B. (1996) *Oncogene* **12**, 1577–1581
36. Cichowski, K., Brugge, J. S., and Brass, L. F. (1996) *J. Biol. Chem.* **271**, 7544–7550
37. Bar-Sagi, D., Rotin, D., Batzer, A., Mandiyan, V., and Schlessinger, J. (1993) *Cell* **74**, 83–91
38. Labeit, S., and Kolmerer, B. (1995) *J. Mol. Biol.* **248**, 308–315
39. Jung, G., Saxe, C. L., 3rd, Kimmel, A. R., and Hammer, J. A., 3rd (1989) *Proc. Natl. Acad. Sci. U. S. A.* **86**, 6186–6190
40. Drubin, D. G., Mulholland, J., Zhu, Z. M., and Botstein, D. (1990) *Nature* **343**, 288–290
41. Wu, H., and Parsons, J. T. (1993) *J. Cell Biol.* **120**, 1417–1426
42. Songyang, Z., Carraway, K. L. R., Eck, M. J., Harrison, S. C., Feldman, R. A., Mohammadi, M., Schlessinger, J., Hubbard, S. R., Smith, D. P., Eng, C., Lorenzo, M. J., Pnder, B. A. J., Mayer, B. J., and Cantley, L. C. (1995) *Nature* **373**, 536–539
43. Ren, R., Mayer, B. J., Cicchetti, P., and Baltimore, D. (1993) *Science* **259**, 1157–1161
44. Vagne-Descroix, M., Pansu, D., Jornvall, H., Carlquist, M., Guignard, H., Jourdan, G., Desvigne, A., Collinet, M., Caillet, C., and Mutt, V. (1991) *Eur. J. Biochem.* **201**, 53–59
45. Sanger, J. M., Mittal, B., Pochapin, M., and Sanger, J. W. (1986) *J. Cell Sci. Suppl.* **5**, 17–44
46. Hamasaki, K., Mimura, T., Morino, N., Furuya, H., Nakamoto, T., Aizawa, S., Morimoto, C., Yazaki, Y., Hirai, H., and Nojima, Y. (1996) *Biochem. Biophys. Res. Commun.* **222**, 338–343
47. Hall, A. (1994) *Annu. Rev. Cell Biol.* **10**, 31–54
48. Zigmond, S. H. (1996) *Curr. Biol.* **8**, 66–73
49. Masaki, T., Endo, M., and Ebashi, S. (1967) *J. Biochem. (Tokyo)* **62**, 630–632
50. Goll, D. E., Dayton, W. R., Singh, I., and Robson, R. M. (1991) *J. Biol. Chem.* **266**, 8501–8510
51. Keller, T. C., 3rd (1995) *Curr. Opin. Cell Biol.* **7**, 32–38
52. Casella, J. F., Craig, S. W., Maack, D. J., and Brown, A. E. (1987) *J. Cell Biol.* **105**, 371–379
53. Koteliansky, V. E., Glukhova, M. A., Gneushev, G. N., Samuel, J. L., and Rappaport, L. (1986) *Eur. J. Biochem.* **156**, 619–623
54. Mittal, B., Sanger, J. M., and Sanger, J. W. (1987) *Cell Motil. Cytoskeleton* **8**, 345–359
55. Moncman, C. L., and Wang, K. (1995) *Cell Motil. Cytoskeleton* **32**, 205–225

BNSDOCID: <XP___2136343A__I_>